Mineralia Slovaca, Web ISSN 1338-3523, ISSN 0369-2086
51 (2019), 61 – 78, © Authors 2019. CC BY 4.0

Mineralogy and geochronology of calc-alkaline lamprophyres from the Nízke Tatry Mts. crystalline complex (Western Carpathians)

JÁN SPIŠIAK[1], LUCIA VETRÁKOVÁ[1], TOMÁŠ MIKUŠ[2], DAVID CHEW[3], ŠTEFAN FERENC[1], VIERA ŠIMONOVÁ[1] and PAVOL SIMAN[2]

[1] Matej Bel University, Faculty of Natural Sciences, Tajovského 40, SK-97401 Banská Bystrica, Slovak Republic; jan.spisiak@umb.sk
[2]Slovak Academy of Sciences, Earth Science Institute, Dúbravská cesta 9, SK-840 05 Bratislava, Slovak Republic
[3]University of Dublin, Trinity College Dublin, College Green, Dublin 2, Ireland

Abstract: The examined Late Paleozoic calc-alkaline dyke rocks occur within the Nízke Tatry Mts. crystalline complex (Kumštová valley and Jarabá village). Their mineral composition is quite simple – the main mafic minerals are clinopyroxene, amphibole and biotite, and the felsic minerals are alkaline feldspar, plagioclase and quartz. They show a rather high degree of alteration. According to their mineralogical composition, the studied rocks correspond to calc-alkaline lamprophyres having revealed and age of 259. 0 ± 2.8 Ma.

Key words: mineralogy, geochemistry, U-Pb dating, lamprophyres, Nízke Tatry Mts.

Graphical abstract

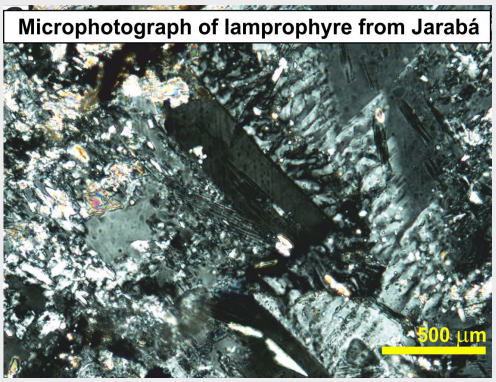

Highlights

- Studied lamprophyre rocks from southern slopes of the Nízke Tatry Mts. are classified as kersantites and spessartites.
- Similarity of their mineral and chemical composition with Permian volcanics of the Hronicum and revealed age 259.0 ± 2.8 Ma point to a possible co-magmatism of these rocks.

Introduction

Lamprophyres represent the dyke rocks, whose mineral composition, structure and chemical composition are different from plutonic and volcanic rocks. Within the Western Carpathian Tatricum and Veporicum crystalline basement, the calc-alkaline dykes occur in the Malé Karpaty Mts., Strážovské vrchy Mts., Malá Fatra Mts., Nízke Tatry Mts. and Veporic Kohút zone. They form a heterogeneous rock group usually classified as quartz porphyrites or lamprophyres (Hovorka, 1967). In the crystalline basement, the dyke rocks were firstly reported by Kamenický (1962) and Krist (1967) in the area of Jarabá and Mýto pod Ďumbierom villages and subsequently described in more details by Hovorka (1967). In the Central Europe, the calc-alkaline lamprophyres typically occur within the granite/granitoid, gneissic and gabbroic rocks – they are represented by minettes, kersantites and spessartites in the Krupka locality, Krušné hory Mts. (Czech Republic; Štemprok et al., 2014; Ulrich et al., 1993), spessartites in Lusatia (Germany; Abdelfadil et al., 2013), kersantites and spessartites in the Erzgebirge (Germany; Seifert, 2008), and in the Sudetes (Poland) with the occurrences of all types of these rocks (Awdankiewicz, 2007). In the French Massif Central, calc-alkaline lamprophyres are represented by kersantites and minettes (Turpin et al., 1988). The age of calc-alkaline lamprophyres from Central Europe is Late-Variscan: French Massif Central (290-315 Ma), Lusatia (ca 330 Ma), Erzgebirge (300-330 Ma), Sudetes (ca 300 Ma) and the Black Forest (314-332 Ma; Hegner et al., 1998). The different extent of enrichment of Late-Variscan lamprophyres in different domains of Central Europe reflects the regional heterogeneous effect of the Variscan orogeny. In this paper, we pay special attention to the chemical composition and the age of the examined minerals.

Geological position

Dykes of calc-alkaline lamprophyres are rather rare in the Western Carpathians. In the eastern part of the Nízke Tatry Mts., lamprophyres occur in several localities (Kamenický, 1962; Krist, 1967). We have focused our research on two best outcropped localities from the wider surroundings of the Jarabá village (Fig. 1). One dyke is cropping out at the mouth of the Kumštová dolina valley to the Jarabá–Čertovica road (N 48° 54′ 19″, E 19° 42′ 14″). The outcrop is located on the left side of the valley. The dyke is 60 – 80 cm thick and is made up of fine-grained kersantite. The host rocks are formed by banded and augen textures (prevailingly mylonitized with abundant amphibolite lenses). The second dyke is cropping out near the village of Jarabá. It is an abandoned quarry approximately in the middle of the village, on the left bank of the brook, on the western slope of the Mlynárska hill (1051.5; N 48° 53′ 25″, E 19° 41′ 39″). The dyke body is uncovered here in a length of about 20 m. It is cropping out in a thickness of at least 5 m. The host rocks are diaphtorized biotite gneisses. The rims of the body are finer grained. Coarse grained kersantite is cropping out in the southern part of the quarry. The lamprophyres are rather highly altered.

Analytical methods

The 18 thin sections were studied with a NIKON Eclipse LV 100N microscope. Silicates and apatites were studied using electron microprobe JEOL JXA 8530FE at Earth Sciences Institute of the Slovak Academy of Sciences in Banská Bystrica under the following conditions for silicates: accelerating voltage 15 kV, probe current 20 nA, beam diameter 3-8 μm, ZAF correction, counting time 10 s on peak, 5 s on background. The used standards, X-ray lines and D.L. (in ppm) were: Ca(Kα, 25) – diopside, K (Kα, 44) – orthoclase, P (Kα, 41) – apatite, F (Kα, 167) – fluorite, Na (Kα, 43) – albite, Mg (Kα, 41) – diopside, Al (Kα, 42) – albite, Si (Kα, 63) – quartz, Ba (Lα, 72) – barite, Fe (Kα, 52) – hematite, Cr (Kα, 113) – Cr_2O_3, Mn (Kα, 59) – rhodonite, Ti (Kα, 130) – rutile, Cl (Kα, 12) – tugtupite, Sr (Lα, 71) – celestite. Following conditions were used for apatites: accelerating voltage 15 kV, probe current 20nA and beam diameter 5 μm and ZAF matrix correction. The EPMA was calibrated by the natural and synthetic standards. Used standards, X-ray lines, crystal and D.L. (in ppm) are: Ca (Kα, PETL, 24-62) - diopside, K (Kα, PETL, 20-48) – orthoclase, Th (Mα, PETL, 41-75) – thorianite, Pb (Mβ, PETL, 65-138) – crocoite, Cl (Kα, PETL, 11-12) – tugtupite, P (Kα, PETL, 56-85) – apatite, S (Kα, PETL, 27-47) – barite, Y – (Lα, PETL, 59-122) – YPO_4, F (Kα, LDE1, 103-273) – fluorite, Na (Kα, TAP, 46-78) – albite, Sr (Lα, TAP, 38-201) – celestite, Si (Kα, TAP, 50-125) – orthoclase, Al (Kα, TAP, 37-100) – albite, Mg (Kα, TAP, 37-87) – diopside, Sm (Lβ, LIFH, 62-274) – $SmPO_4$, Pr (Lβ, LIFH, 121-235) – $PrPO_4$, Nd (Lα, LIFH, 62-123) – $NdPO_4$, Ce (Lα, LIFH, 65-129) – $CePO_4$, La (Lα, LIFH, 72-139) – $LaPO_4$, Fe (Kα, LIF, 94-333) – hematite, Mn (Kα, LIF, 79-238) – rhodonite, Ti (Kα, LIF, 133-333) – rutile, Ba (Lα, LIF, 242-674) – barite.

Apatite crystals were separated using standard techniques. Apatite U-Pb data were acquired using a Photon Machines Analyte Exite 193 nm ArF Excimer laser-ablation system coupled to a Thermo Scientific iCAP Qc at the Department of Geology, Trinity College Dublin. Twenty-eight isotopes (^{31}P, ^{35}Cl, ^{43}Ca, ^{55}Mn, ^{86}Sr, ^{89}Y, ^{139}La, ^{140}Ce, ^{141}Pr, ^{146}Nd, ^{147}Sm, ^{153}Eu, ^{157}Gd, ^{159}Tb, ^{163}Dy, ^{165}Ho, ^{166}Er, ^{169}Tm, ^{172}Yb, ^{175}Lu, ^{200}Hg, ^{204}Pb, ^{206}Pb, ^{207}Pb, ^{208}Pb, ^{232}Th, ^{238}U and mass ($^{248/232}Th$ ^{16}O) were acquired using a 50 μm laser spot, a 4 Hz laser repetition rate and a fluence of 3.31 J/cm^2. A ca 1 cm sized crystal of Madagascar apatite, which has yielded a weighted average ID-TIMS concordia age of 473.5± 0.7 Ma (Thomson et al., 2012; Cochrane et al., 2014), was used as a primary apatite reference material in this study. McClure Mountain syenite apatite (the rock from which the $^{40}Ar/^{39}Ar$ hornblende standard MMhb is derived) was used as a secondary standard. McClure Mountain syenite has moderate but reasonably consistent U and Th contents (~23 ppm and 71 ppm – Chew & Donelick, 2012) and its thermal history, crystallization age (weighted mean $^{207}Pb/^{235}U$ age of 523.51 ± 2.09 Ma) and initial Pb isotopic composition ($^{206}Pb/^{204}Pb = 17.54 \pm 0.24$; $^{207}Pb/^{204}Pb = 15.47 \pm 0.04$) are known from high-precision TIMS analyses (Schoene & Bowring, 2006). Durango apatite was also analysed in this study as a secondary standard. Durango apatite is a distinctive yellow-green fluorapatite widely used as a mineral standard in apatite fission-track and (U-Th)/He dating and apatite electron micro-probe analyses. It is found in the form of large crystals within an open pit iron mine at Cerro de Mercado, Durango, Mexico. The apatite formed between the eruptions of two major ignimbrites, yielding a sanidine-anorthoclase ^{40}Ar-^{39}Ar age of 31.44 ± 0.18 Ma (McDowell et al., 2005). NIST 612 standard glass was used as the apatite trace element concentration reference material. The raw isotope data were reduced using the "VisualAge" data reduction scheme of Petrus & Kamber (2012) within the freeware IOLITE package of Paton et al. (2011). User-defined time intervals are established for the baseline correction procedure to calculate session-wide baseline-corrected values for each isotope. The time-resolved fractionation response of individual standard analyses is then characterized using a user-specified down-hole correction model (such as an exponential curve, a linear fit or a smoothed cubic spline). The data reduction scheme then fits this appropriate sessionwide "model" U-Th-Pb fractionation curve to the time-resolved standard data and the unknowns. Sample-standard bracketing is applied after the correction of down-hole fractiona-

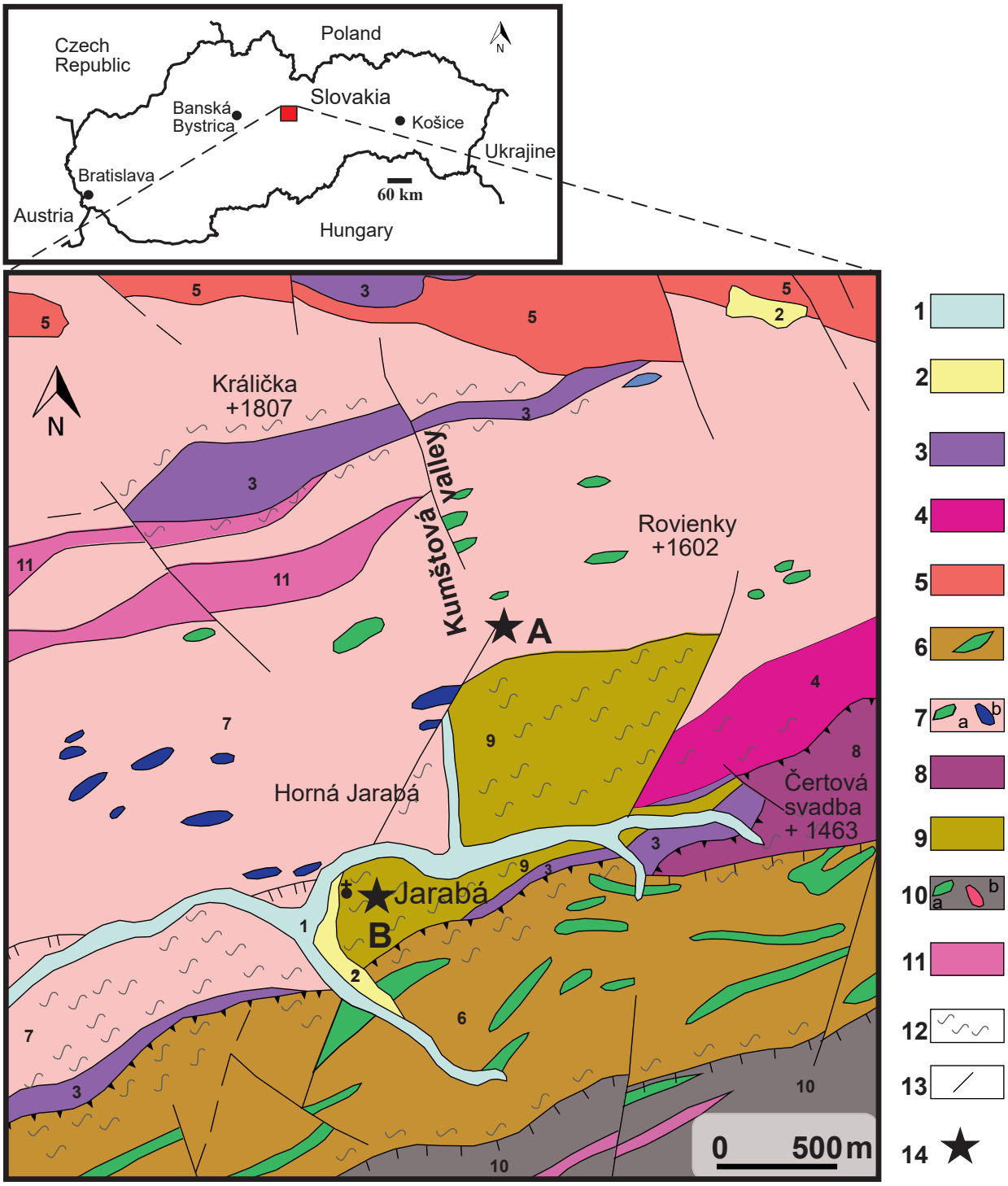

Fig. 1. Geological map of a part of the Nízke Tatry Mts. (Digital geological map of the Slovak Republic at scale 1 : 50 000 [online]. State Geological Institute of Dionýz Štúr, Bratislava, 2013). Legend: Quaternary: 1 - fluvial sediments, 2 - deluvial sediments; Early Triassic: 3 - Lúžňa Formation; Late Paleozoic: 4 - biotite granodiorites to tonalites (Ďumbier type), 5 - biotite and two-mica granites (Králička type); Early Paleozoic: 6 - garnet-muscovite-biotite paragneisses, mica schist gneisses to mica schists with rock body of amphibolites, 7 - biotite and muscovite-biotite gneisses with banded structure with rock body of: a - amphibolites, b - porphyrites, lamprophyres; 8 - K-feldspar-plagioclase gneisses and synkinematic, banded migmatites, 9 - biotite paragneisses, 10 - chlorite-sericite phyllites with rock body of (a) metamorphites of volcanics and volcaniclastics of basic composition, (b) metamorphites of volcanics and volcaniclastics of rhyodacitic and dacitic composition, 11 - orthogneisses (Struhár type). 12 - mylonite zones, 13 - fault lines, 14 - samples (A = Kum-1, 2, 3; B = Jar-1, 2, 3, 4).

tion to account for long-term drift in isotopic or elemental ratios by normalizing all ratios to those of the U-Pb reference standards. Common Pb in the apatite standards was corrected using the ^{207}Pb-based correction method using a modified version of the VisualAge DRS that accounts for the presence of variable common Pb in the primary standard materials (Chew et al., 2014). Over the course of two months of analyses, McClure Mountain apatite (^{207}Pb/^{235}U TIMS age of 523.51 ± 1.47 Ma, (Schoene & Bowring, 2006) yielded a U-Pb Tera-Wasserburg concordia lower intercept age of 524.5 ± 3.7 Ma with an MSWD = 0.72. The lower intercept was anchored using a ^{207}Pb/^{206}Pb value of 0.88198, derived from an apatite ID-TIMS total U-Pb isochron (Schoene & Bowring, 2006).

The structural formulas of clinopyroxenes, biotites and feldspars were recalculated using the Mineral Formulae Recalculation. The mineral recalculation is accessible on the (web:https://serc.carleton.edu/research_education/equilibria/mineralformulaerecalculation.html). The structural formulas of amphiboles were recalculated using the Amphibole Classification (Locock, https://github.com/AndrewLocock/Amphibole/releases/tag/1.9.3).

Mineralogy and petrology

Lamprophyre rocks from the Jarabá wider surroundings are grey-black in colour, have a fine-grained to aphanitic groundmass and medium to fine-grained texture. In coarser grained varieties, thin lamellae of clinopyroxene, and/or amphibole can be observed. The mineral composition of the rocks in two localities is different in modal abundance of dark minerals (especially biotite, amphibole and pyroxene), biotite is prevailing in the Kumštová dolina valley, whereas in Jarabá it is mostly clinopyroxene and amphibole. The modal composition of the rocks is also reflected in their classification. Based on IUGS classification (LeMaitre et al., 2002; Ondrejka et al., 2015), the examined dyke rocks from the Nízke Tatry Mts. belong to kersantite (Kumštová dolina; plagioclase > K-feldspar, biotite > amphibole and clinopyroxe), and/or spessartite (Jarabá, plagioclase > K-feldspar, amphibole and clinopyroxene). Besides primary minerals (clinopyroxene, amphibole, biotite, feldspar and quartz), the lamprophyres under study often contain also secondary minerals (chlorite, epidote and carbonates). From ore minerals there are dominating magnetite, Fe-Ti rutile, hematite and pyrite, and in accessory amounts there occur apatite and zircon. The rocks are characteristic with strongly altered primary minerals, notably clinopyroxene, amphibole, biotite as well as plagioclase.

Clinopyroxenes represent the main rock forming minerals (Tab. 1). They were observed only in the Jarabá locality. They are often enclosing amphiboles (Fig. 2a, b) and based on Morimoto et al. (1988) classification, their chemical composition corresponds to augite (Fig. 3).

Several types of amphiboles occur in examined rocks. All they are strongly altered – chloritized (Fig. 2a, b). There are frequent occurrences of older (lighter) amphiboles with a high FeO, Na_2O and a low MgO and CaO contents enclosed by younger (darker) amphiboles with a lower FeO and Na_2O and a higher MgO and CaO contents (Fig.4a, Tab. 2). Generally, the studied amphiboles are characteristic for a low TiO_2 content. Based on IMA classification (Hawthorne et al., 2012), the amphiboles can be classified as Ca-amphiboles, tremolites (Fig. 5). From the composition and occurrences of the amphiboles it is very likely that their current composition was strongly influenced by alteration processes and the composition of the primary amphiboles, co-existing with clinopyroxenes, was different. In the Kumštová dolina valley, there were found only pseudomorphoses after amphiboles mostly filled with chlorite.

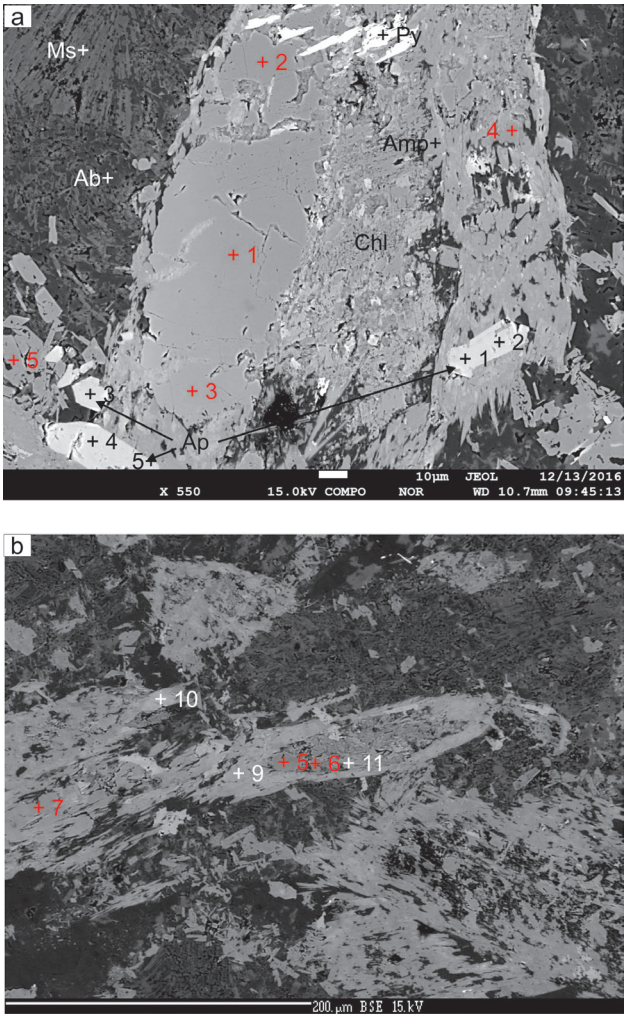

Fig. 2. Back scattered electron (BSE) images of lamprophyre, Ab - albite, Amp - amphibole, Ap - apatite, Ms – muscovite, Py – pyrite, Chl - chlorite. The numbers in figures correspond to those in Table 1 and Table 6. Locality: Jarabá.

Tab. 1.
Selected analyses of clinopyroxenes.

sample	JAR-1							
figure	Fig. 2a	Fig. 2a	Fig. 2a	Fig. 2a	Fig. 2b	Fig. 2b	Fig. 2b	Fig. 2b
N. anal.	1	2	3	4	5	6	7	8
SiO_2	51.63	51.54	51.61	52.63	51.26	51.01	50.07	50.96
TiO_2	1.30	1.34	0.90	1.16	1.14	1.04	1.39	1.12
Al_2O_3	2.39	2.67	2.01	2.35	2.23	2.06	2.27	2.33
Cr_2O_3	0.11	0.00	0.01	0.00	0.05	0.05	0.00	0.03
FeO*	10.87	9.41	13.48	10.09	9.91	10.08	12.89	10.91
MnO	0.31	0.26	0.32	0.25	0.25	0.28	0.37	0.29
MgO	13.65	14.18	12.31	14.31	14.86	14.88	13.48	15.17
CaO	19.24	19.70	18.95	18.51	19.60	19.66	18.80	18.86
Na_2O	0.13	0.15	0.11	0.15	0.35	0.24	0.28	0.22
K_2O	0.00	0.00	0.00	0.00	0.02	0.05	0.04	0.01
Sum	99.64	99.24	99.70	99.45	99.68	99.35	99.57	99.90
Formula based on 6 oxygens								
Si	1.947	1.939	1.965	2.052	1.914	1.913	1.895	1.902
Ti	0.037	0.038	0.026	0.032	0.032	0.029	0.040	0.031
Al	0.106	0.118	0.090	0.100	0.098	0.091	0.101	0.102
Cr	0.003	0.000	0.000	0.000	0.001	0.001	0.000	0.001
Fe^{3+}	0.000	0.000	0.000	0.000	0.033	0.039	0.049	0.046
Fe^{2+}	0.343	0.296	0.429	0.306	0.276	0.277	0.359	0.294
Mn	0.010	0.008	0.010	0.008	0.008	0.009	0.012	0.009
Mg	0.767	0.795	0.699	0.773	0.827	0.832	0.761	0.844
Ca	0.777	0.794	0.773	0.719	0.784	0.790	0.763	0.754
Na	0.010	0.011	0.008	0.010	0.025	0.017	0.021	0.016
X (Wol) %	41.179	42.114	40.664	39.978	40.824	40.761	39.481	38.900
X (En) %	40.664	42.177	36.762	43.010	43.065	42.926	39.389	43.536
X (Fs) %	18.157	15.709	22.574	17.012	16.111	16.313	21.129	17.564

FeO* total Fe as FeO

Tab. 2.
Selected analyses of amphiboles.

Sample	JAR-1								
Figure	Fig. 2b	Fig. 2b	Fig. 2b	Fig. 4a	Fig. 4a	Fig. 4a	Fig. 4a	Fig. 4a	Fig. 4a
N. anal.	9	10	11	12	13	14	15	16	17
SiO_2	48.89	48.75	49.85	48.68	48.49	49.25	49.68	50.05	50.71
TiO_2	0.11	0.12	0.28	0.15	0.18	0.09	0.05	0.00	0.05
Al_2O_3	4.09	3.07	3.64	2.02	2.18	1.50	3.26	2.75	3.15
Cr_2O_3	0.01	0.00	0.03	0.00	0.01	0.02	0.00	0.01	0.00
FeO*	22.13	24.26	19.04	32.35	32.20	31.86	23.35	24.42	23.03
MnO	0.31	0.69	0.22	0.61	0.62	0.75	0.34	0.42	0.39
MgO	8.30	9.12	10.89	3.47	3.48	3.87	8.21	7.60	8.33
CaO	12.03	8.03	10.88	9.38	9.34	9.59	12.03	11.85	11.89
Na_2O	0.50	1.25	0.26	0.94	0.87	0.76	0.32	0.28	0.17
K_2O	0.28	0.29	0.94	0.22	0.24	0.27	0.28	0.24	0.64
Sum	96.67	95.67	96.03	97.82	97.62	97.96	97.50	97.62	98.35

Tab. 2 – continuation.

Sample	JAR-1								
Figure	Fig. 2b	Fig. 2b	Fig. 2b	Fig. 4a	Fig. 4a	Fig. 4a	Fig. 4a	Fig. 4a	Fig. 4a
N. anal.	9	10	11	12	13	14	15	16	17
Formula based on 24 (OH.F.Cl.O)									
Si	7.489	7.532	7.569	7.673	7.659	7.745	7.555	7.636	7.649
Al^{IV}	0.511	0.468	0.431	0.327	0.341	0.255	0.445	0.364	0.351
Al^{VI}	0.228	0.091	0.221	0.049	0.065	0.023	0.139	0.130	0.208
Ti	0.013	0.013	0.032	0.018	0.022	0.011	0.006	0.000	0.005
Fe^{3+}	0.081	0.400	0.024	0.291	0.272	0.235	0.188	0.172	0.036
Fe^{2+}	2.755	2.734	2.393	3.974	3.982	3.955	2.781	2.944	2.869
Mn	0.040	0.090	0.028	0.081	0.083	0.100	0.018	0.030	0.042
Mg	1.896	2.102	2.464	0.815	0.820	0.907	1.861	1.728	1.873
Ca	1.975	1.328	1.770	1.583	1.580	1.615	1.961	1.936	1.921
Na	0.149	0.374	0.077	0.286	0.267	0.232	0.094	0.084	0.050
K	0.055	0.058	0.182	0.045	0.048	0.054	0.054	0.046	0.123

FeO* total Fe as FeO

Tab. 3.
Selected analyses of biotites.

sample	KUM-1			KUM-2			
figure	Fig. 4b	Fig. 4b	Fig. 4b				
N. anal.	1	2	3	4	5	6	7
SiO_2	36.83	35.03	36.18	36.27	36.89	35.83	36.48
TiO_2	4.14	3.36	4.00	4.67	3.65	3.49	4.02
Al_2O_3	12.29	13.37	12.91	12.29	12.39	14.34	13.07
Cr_2O_3	0.02	0.00	0.00	0.00	0.02	0.00	0.00
FeO*	23.61	25.22	24.21	25.12	24.50	23.68	23.55
MnO	0.11	0.16	0.14	0.12	0.15	0.08	0.21
MgO	9.02	10.79	9.39	8.06	9.23	9.61	9.44
CaO	0.10	0.24	0.04	0.06	0.07	0.07	0.08
Na_2O	0.03	0.12	0.06	0.13	0.08	0.03	0.04
K_2O	8.94	6.62	8.30	8.98	8.68	7.76	8.12
Sum	95.10	94.90	95.23	95.71	95.66	94.89	95.01
Formula based on 24 oxygens							
Si	5.755	5.479	5.647	5.685	5.745	5.513	5.604
Al^{IV}	2.245	2.465	2.353	2.271	2.255	2.487	2.367
Al^{VI}	0.019	0.000	0.022	0.000	0.019	0.114	0.000
Ti	0.487	0.395	0.469	0.551	0.428	0.404	0.464
Fe	3.086	3.299	3.160	3.293	3.191	3.047	3.025
Mn	0.015	0.022	0.018	0.016	0.020	0.011	0.027
Mg	2.102	2.516	2.185	1.884	2.142	2.204	2.162
Ca	0.017	0.040	0.006	0.010	0.012	0.011	0.013
Na	0.010	0.036	0.019	0.041	0.025	0.009	0.011
K	1.782	1.320	1.652	1.795	1.725	1.524	1.591
Al total	2.263	2.465	2.376	2.271	2.274	2.601	2.367
Fe/Fe+Mg	0.595	0.567	0.591	0.636	0.598	0.580	0.583

FeO* total Fe as FeO

Tab. 4.
Selected analyses of plagioclases.

sample	KUM-2		KUM-1					JAR-1
figure	Fig. 8a	Fig. 8a	Fig. 8b	Fig. 8b	Fig. 8b	Fig. 8b	Fig. 8b	
N. anal.	1	2	3	4	5	6	7	8
SiO_2	59.83	55.20	54.92	64.58	56.25	58.12	58.09	66.51
TiO_2	0.00	0.00	0.00	0.00	0.00	0.00	0.00	0.07
Al_2O_3	24.91	27.64	27.45	21.27	26.74	25.63	24.94	20.70
Cr_2O_3	0.00	0.00	0.00	0.00	0.00	0.00	0.00	0.05
FeO*	0.34	0.40	0.38	0.14	0.44	0.35	0.31	0.12
MnO	0.00	0.00	0.00	0.00	0.00	0.00	0.00	0.08
MgO	0.00	0.06	0.00	0.00	0.03	0.00	0.03	0.00
CaO	7.31	11.09	11.18	3.63	9.90	8.65	9.28	1.18
Na_2O	6.53	4.75	4.79	8.14	5.44	5.91	5.82	10.32
K_2O	1.05	0.53	0.53	1.59	0.65	0.81	0.74	0.18
Sum	99.98	99.68	99.25	99.36	99.45	99.47	99.21	99.19
Formula based on 8 oxygens								
Si	2.688	2.513	2.507	2.897	2.553	2.633	2.641	2.952
Ti	0.000	0.000	0.000	0.000	0.000	0.000	0.000	0.002
Al	1.318	1.482	1.477	1.124	1.430	1.368	1.337	1.083
Cr	0.000	0.000	0.000	0.000	0.000	0.000	0.000	0.002
Fe^{3+}	0.000	0.000	0.000	0.000	0.000	0.000	0.000	0.000
Fe^{2+}	0.013	0.015	0.015	0.005	0.017	0.013	0.012	0.004
Mn	0.000	0.000	0.000	0.000	0.000	0.000	0.000	0.003
Mg	0.000	0.000	0.000	0.000	0.002	0.000	0.002	0.000
Ca	0.352	0.541	0.547	0.174	0.481	0.420	0.452	0.056
Ba	0.000	0.000	0.000	0.000	0.000	0.000	0.000	0.000
Na	0.569	0.419	0.424	0.708	0.479	0.519	0.513	0.888
K	0.060	0.031	0.031	0.091	0.038	0.047	0.043	0.010
X (An) %	35.874	54.585	54.592	17.923	48.250	42.591	44.846	5.880
X (Ab) %	57.991	42.308	42.326	72.730	47.978	52.660	50.896	93.053
X (Or) %	6.135	3.106	3.082	9.348	3.772	4.749	4.258	1.068

FeO* total Fe as FeO

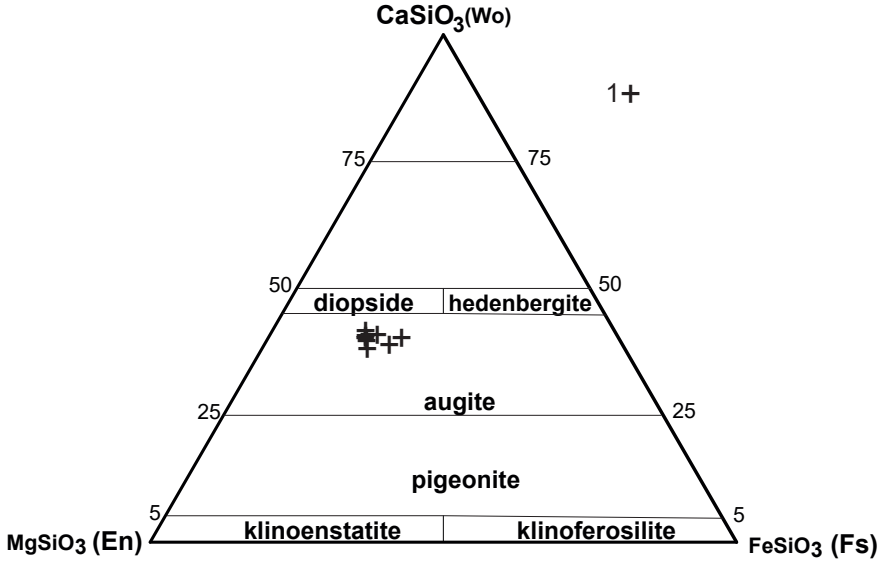

Fig. 3. The classification diagram of pyroxenes, according Morimoto et al. (1988), 1 - clinopyroxene from Jarabá.

Tab. 5.
Selected analyses of K-feldspars.

Sample	JAR-1			KUM- 2		KUM- 1			JAR-1		
Figure	Fig. 4a	Fig. 4a	Fig. 4a	Fig. 8a	Fig. 8a	Fig. 8b	Fig. 8b	Fig. 8b	Fig. 8c	Fig. 8c	Fig. 8c
N. anal.	1	2	3	4	5	6	7	8	9	10	11
SiO_2	59.81	61.19	64.18	62.78	64.63	64.86	64.75	64.10	61.83	62.50	64.05
TiO_2	0.00	0.00	0.00	0.00	0.00	0.00	0.00	0.00	0.00	0.00	0.00
Al_2O_3	20.48	20.01	19.22	20.15	19.47	19.82	18.77	18.73	19.02	18.94	18.67
Cr_2O_3	0.00	0.00	0.00	0.00	0.00	0.00	0.00	0.00	0.02	0.10	0.00
BaO	5.46	3.67	0.03	1.63	0.10	0.00	0.03	0.00	2.52	2.25	0.04
FeO*	0.25	0.20	0.23	0.21	0.09	0.08	0.11	0.20	0.03	0.04	0.09
MnO	0.00	0.00	0.00	0.00	0.00	0.00	0.00	0.00	0.00	0.04	0.00
MgO	0.00	0.00	0.00	0.00	0.00	0.00	0.00	0.00	0.00	0.00	0.00
CaO	0.06	0.06	0.03	0.47	0.44	0.45	0.07	0.10	0.00	0.00	0.21
Na_2O	0.46	0.29	0.29	1.84	3.30	3.72	0.42	0.55	0.21	0.20	0.19
K_2O	14.08	14.79	16.29	12.88	11.50	10.70	15.55	15.45	15.42	15.79	16.53
Sum	100.60	100.22	100.26	99.96	99.52	99.62	99.69	99.12	99.05	99.85	99.79
Formula based on 8 oxygens											
Si	2.902	2.930	2.961	2.928	2.960	2.959	3.007	2.990	2.963	2.965	2.971
Ti	0.000	0.000	0.000	0.000	0.000	0.000	0.000	0.000	0.000	0.000	0.000
Al	1.171	1.129	1.045	1.107	1.051	1.065	1.027	1.029	1.074	1.059	1.020
Fe	0.010	0.008	0.009	0.008	0.003	0.003	0.004	0.008	0.001	0.002	0.004
Mn	0.000	0.000	0.000	0.000	0.000	0.000	0.000	0.000	0.000	0.001	0.000
Mg	0.000	0.000	0.000	0.000	0.000	0.000	0.000	0.000	0.000	0.000	0.000
Ca	0.003	0.003	0.001	0.023	0.022	0.022	0.004	0.005	0.000	0.000	0.011
Na	0.043	0.027	0.026	0.166	0.292	0.329	0.037	0.049	0.019	0.019	0.017
K	0.871	0.903	0.958	0.766	0.672	0.622	0.921	0.919	0.942	0.955	0.978
X(An) %	0.345	0.339	0.145	2.450	2.194	2.244	0.379	0.517	0.000	0.000	1.062
X(Ab) %	4.708	2.880	2.631	17.414	29.665	33.808	3.885	5.086	1.989	1.914	1.685
X(Or) %	94.947	96.782	97.224	80.136	68.141	63.947	95.736	94.397	97.990	98.086	97.253

FeO* total Fe as FeO

Similar to amphibole, biotite is strongly chloritized. High TiO_2 contents prove its magmatic origin, and at the same time, lower contents of K_2O in analyses point to a high secondary alteration. Biotite is a dominant mineral in kersantites from the Kumštová dolina valley. In Jarabá, only rarely there were found tiny, strongly altered biotites. On the basis of chemical composition (Tab. 3, Fig. 6), we include the studied dark micas into the group of annite (Rieder et al., 1998). We also used a discrimination diagram for biotites from different types of geotectonic environments (Fig. 7; Abdel-Rahman, 1993). In the diagram, the biotites fall within the group of biotites from calc-alkaline rocks, on the boundary with alkaline rocks.

From the felsic minerals, the plagioclase and alkaline feldspar are dominant for the lamprophyric rocks studied. Plagioclases significantly predominate over alkaline feldspars. They are strongly sericitized and often contain albite lamellae. Plagioclases are typical with their zonal structure - their central parts are more basic (An_{36-55}) than the rims (An_{18}) (Tab. 4, Figs. 8 and 9). In the case of alkaline feldspars, in addition to the varying amounts of sodium (Na_2O content up to 3.72%), an increased BaO content is obser-

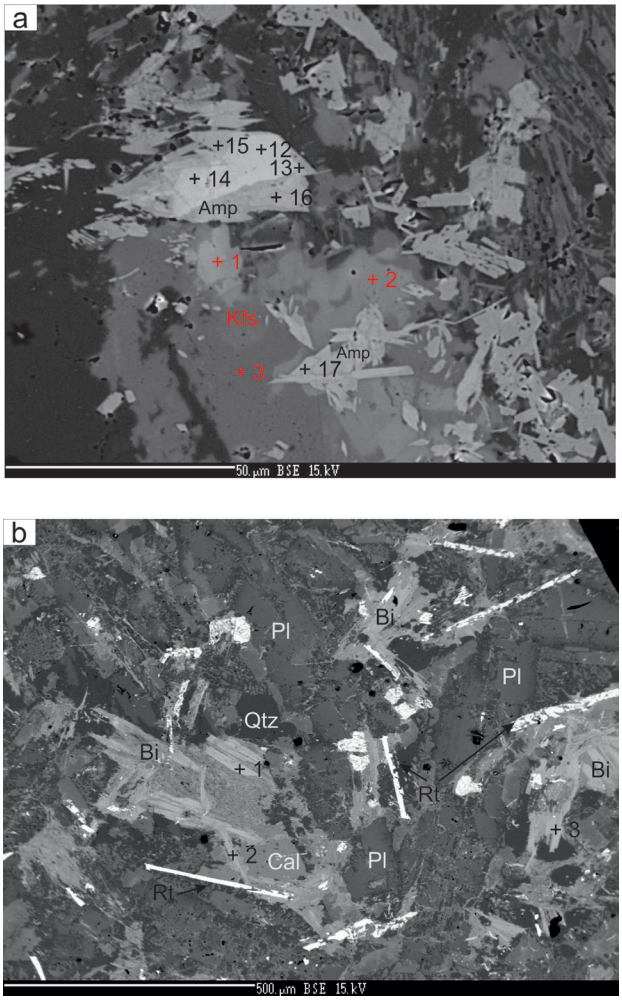

Fig. 4. Back scattered electron (BSE) images of lamprophyre; Pl – plagioclases, Cal – calcite, Qtz – quartz, Rt – rutile, Bt – biotite, Kfs – K-feldspar; the numbers in figures correspond to those in Table 2 and Table 3.

ved. In some cases, the content of BaO is relatively high (5.46 wt.%, Tab. 5). Barium feldspar forms central parts of the grains and the marginal parts are formed by pure potassium feldspar (Figs. 4a and 8c). Quartz in the studied rocks is mostly irregularly restricted, allotriomorphic and often undulous. It is often overgrown with other minerals, especially K-feldspars (Fig. 10). We did not observe xenoliths of individual minerals or fragments of surrounding rocks in the rocks, as was observed in the case of lamprophyres from the Malá Fatra Mts. region (Spišiak et al., 2018).

Apatite is a common and very important accessory mineral in a wide range of igneous rocks. In the rocks studied, apatite occurs as microphenocrysts and in the groundmass it is a very common phase crystallizing at an early stage. It is mostly present in the form of needles (closed in quartz and albite; Fig. 11), or less commonly in the form of short-column shapes (Fig. 2a). The composition of apatite is optically and chemically homogeneous. Fluorine is the dominant anion present in the apatites (Tab. 6) and its content is about 4.0 wt.%. Such high F contents are typical of apatite from lamprophyres with orogenic affinities (e.g., Krmíček et al., 2011; Tappe et al., 2006; Pandey et al., 2017). The content of Cl is very low. Sr content in apatites (Tab. 7) varies around 1500 ppm, which is lower than in orogenic and anorogenic lamprophyres (e.g. Mitchell and Bergman, 1991; Chakhmouradian et al., 2002). In general, Sr content in apatites decreases with magmatic differentiation (e.g. Belousova et al., 2002; Chu et al., 2009). On the contrary, the REE concentration in apatite increases during the evolution from primitive to more-evolved rocks (Ladenburger et al., 2016). REE contents in the studied apatites are rather high (Tab. 7), with a significant enrichment in LREE against HREE. The chondrite-normalized REE curve (Fig. 12) has a sloping course in the direction of decreasing HREE content, and

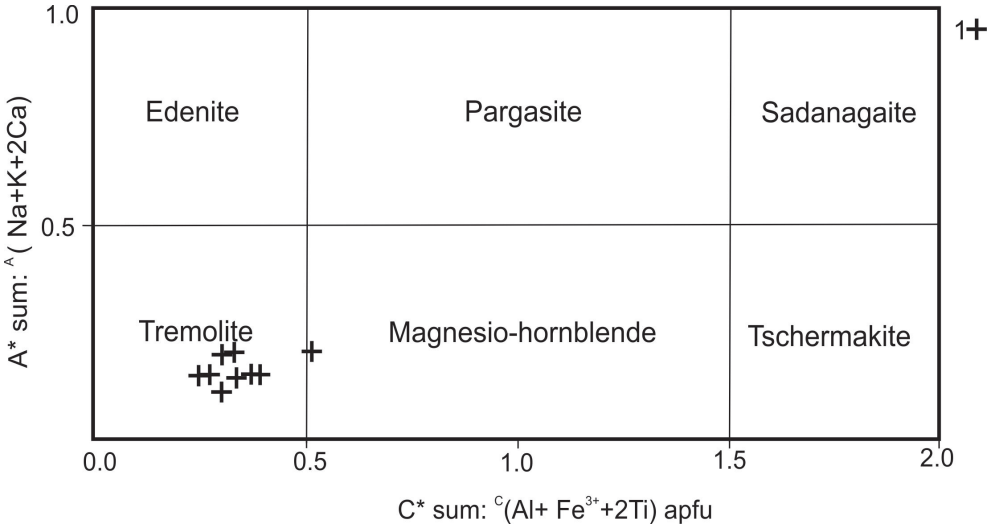

Fig. 5. The classification diagram of amphiboles, according Hawthorne et al. (2012) 1 – amphiboles from Jarabá.

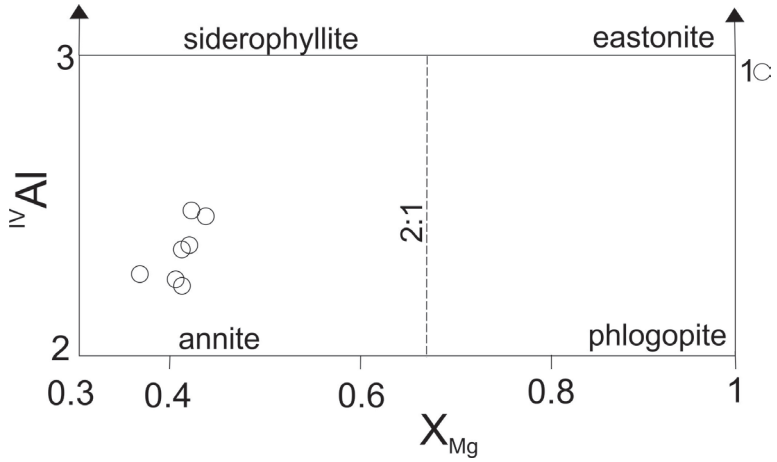

Fig. 6. Classification diagram of studied micas. End-members names according to Rieder et al. (1998), 1 – biotites from Kumštová valley.

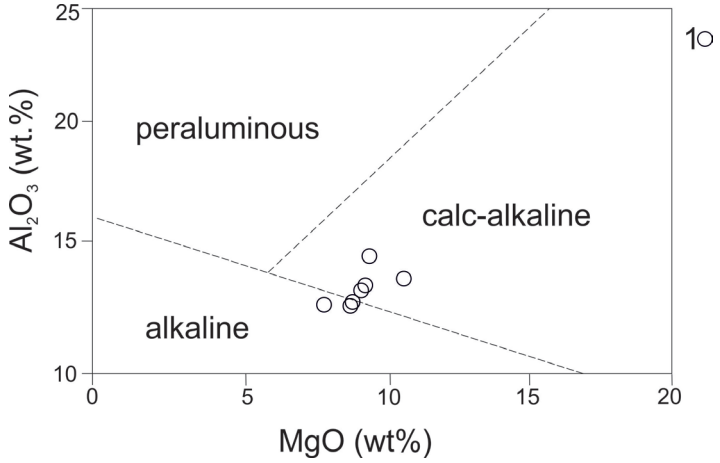

Fig. 7. Position of studied mica in the classification diagram of Abdel-Rahman (1993) for micas from different magmatic series. 1 – biotites from Kumštová valley.

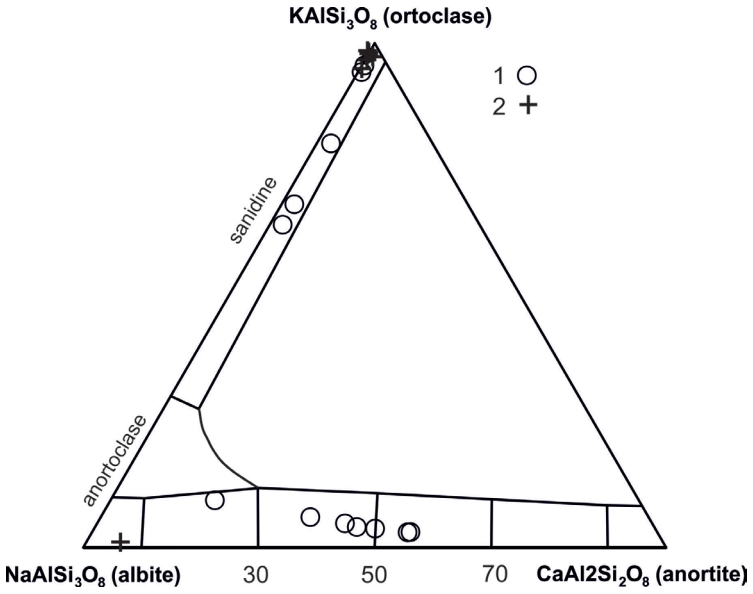

Fig. 9. The classification diagram of feldspars. 1 – Kumštová valley, 2 – Jarabá.

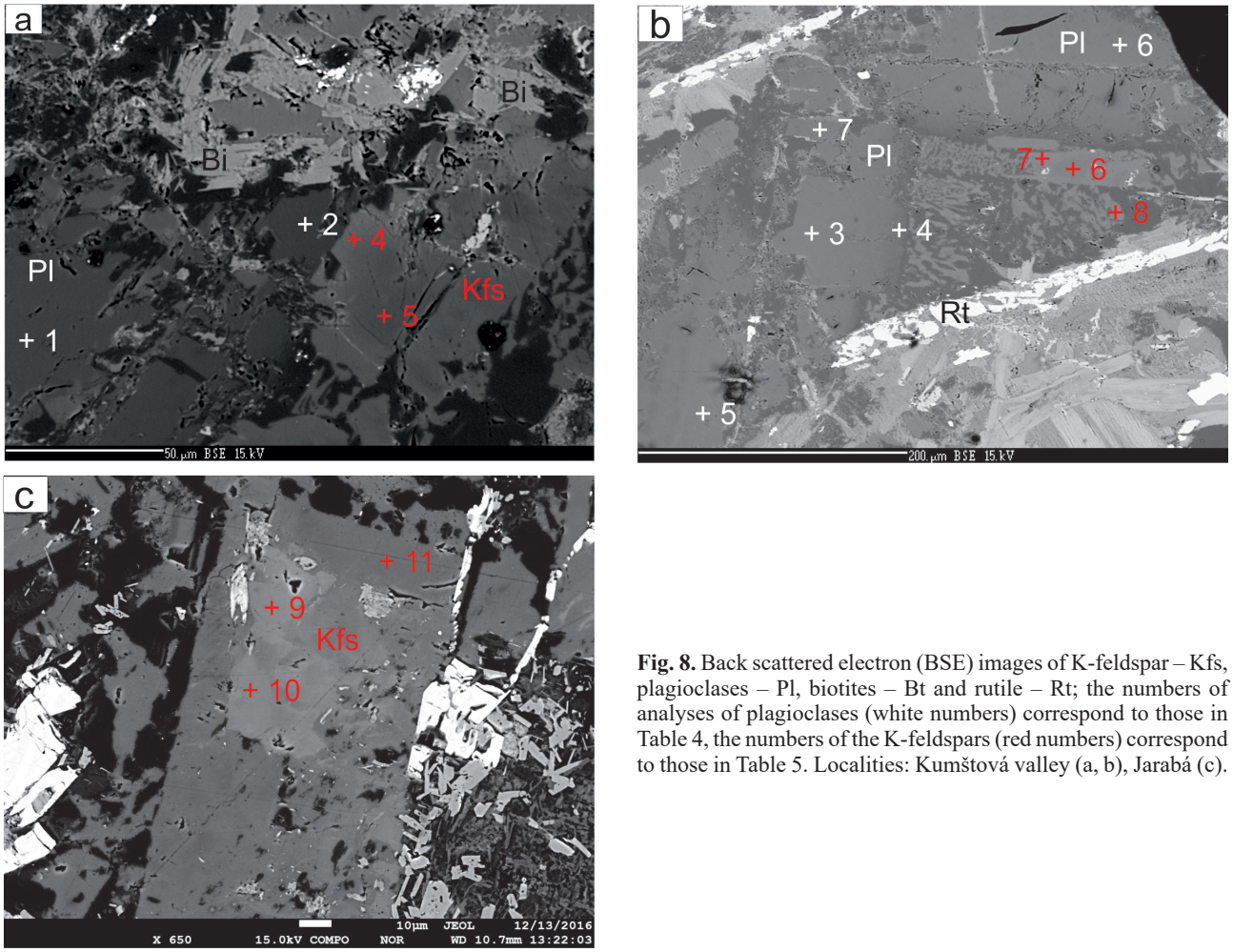

Fig. 8. Back scattered electron (BSE) images of K-feldspar – Kfs, plagioclases – Pl, biotites – Bt and rutile – Rt; the numbers of analyses of plagioclases (white numbers) correspond to those in Table 4, the numbers of the K-feldspars (red numbers) correspond to those in Table 5. Localities: Kumštová valley (a, b), Jarabá (c).

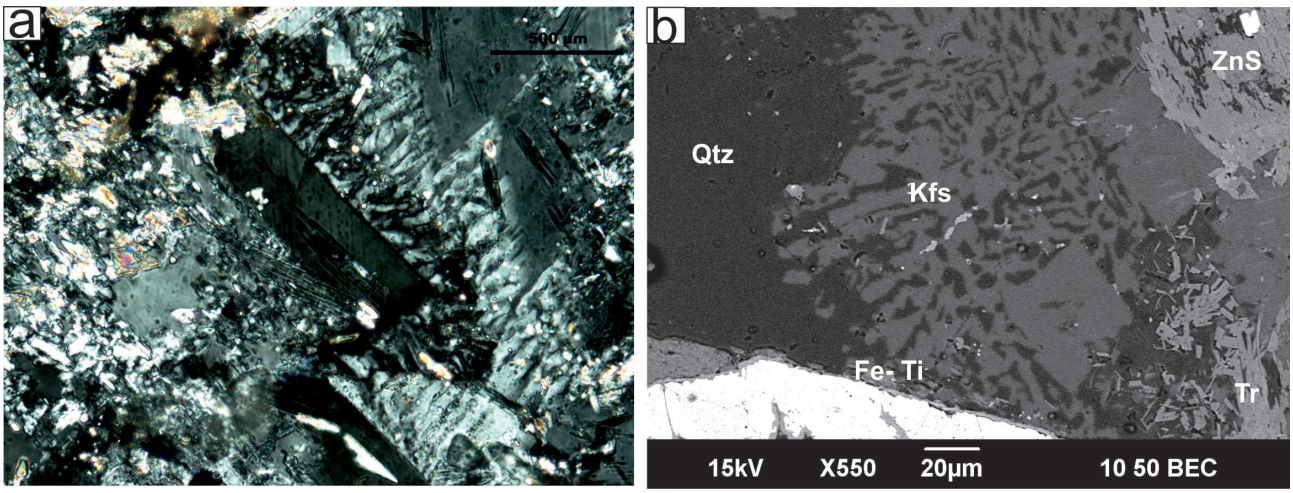

Fig. 10. a – Photomicrograph of lamprophyre; crossed polaroids. b – Back scattered electron (BSE) images of lamprophyres; Kfs – K-feldspar, Qtz – quartz, Tr – tremolite. Locality: Jarabá.

Tab. 6.
The selected microprobe analyses of apatites.

Sample	JAR-1				
Figure	**Fig. 2a**	**Fig. 2a**	**Fig. 2a**	**Fig. 2a**	**Fig. 2a**
N. anal.	**1**	**2**	**3**	**4**	**5**
SiO_2	0.21	0.18	0.19	0.14	0.13
TiO_2	0.02	0.08	0.07	0.03	0.00
Al_2O_3	0.02	0.02	0.02	0.01	0.03
FeO	0.70	0.55	0.73	0.58	0.53
MnO	0.05	0.03	0.07	0.07	0.00
CaO	52.78	52.35	52.87	52.79	52.90
MgO	0.10	0.05	0.06	0.03	0.07
SrO	0.11	0.09	0.15	0.15	0.11
BaO	0.00	0.10	0.03	0.00	0.03
PbO	0.01	0.00	0.00	0.03	0.00
Na_2O	0.00	0.00	0.00	0.00	0.05
K_2O	0.01	0.02	0.03	0.03	0.07
P_2O_5	40.89	41.35	41.09	41.62	41.34
F	3.99	4.01	3.92	3.33	3.19
SO_3	0.02	0.00	0.00	0.01	0.02
ThO_2	0.00	0.00	0.03	0.00	0.01
Y_2O_3	0.28	0.18	0.24	0.27	0.24
Sm_2O_3	0.11	0.01	0.06	0.06	0.07
Pr_2O_3	0.04	0.13	0.06	0.08	0.02
Nd_2O_3	0.36	0.34	0.30	0.30	0.20
Ce_2O_3	0.48	0.41	0.47	0.44	0.37
La_2O_3	0.21	0.17	0.19	0.11	0.16
Total	**100.38**	**100.07**	**100.55**	**100.07**	**99.52**

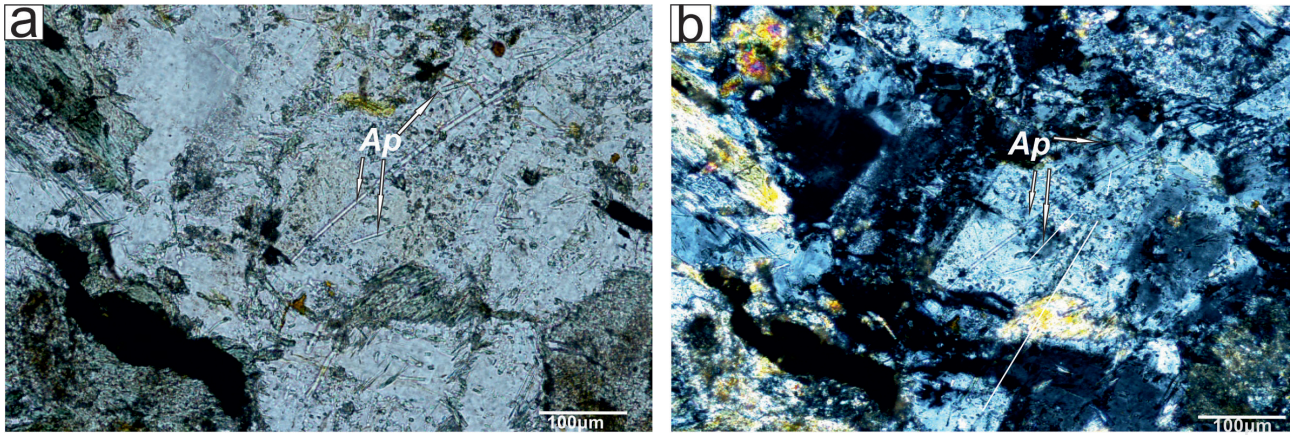

Fig. 11. a – The microphotography of apatite shape (closed in quartz and albite) in lamprophyres, parallel polaroids; b – crossed polaroids. Locality: Jarabá.

Tab. 7.
Representative apatite La-ICP-MS analyses of REE. Y. Pb. Th and U

sample	JAR-1																					
anal. N.	1	2	3	4	5	6	7	8	9	10	11	12	13	14	15	16	17	18	19	20	21	22
La	1309	1327	1303	1297	1307	1282	1299	1289	1289	1299	1301	1275	1307	1313	1281	1268	1257	1270	1255	1298	1303	1277
Ce	2753	2800	2748	2764	2803	2760	2768	2757	2726	2815	2697	2745	2754	2754	2773	2691	2703	2711	2674	2743	2809	2744
Pr	357.4	362.9	354.8	355.9	363	353.1	361	359	349.3	360.7	356	355.6	357.8	356	360.9	351	350.7	351	349.2	357.3	357	348.9
Nd	1438	1444	1431	1441	1453	1420	1450	1447	1421	1455	1439	1421	1446	1445	1443	1412	1411	1415	1378	1441	1448	1407
Sm	234.9	236.1	231.8	233.2	237.3	230.7	233.3	233.8	229.6	236.5	230.3	229.8	234.3	232.4	232.3	228.2	229.1	226.1	223	228.9	233.6	223.9
Eu	43.14	43.35	42.79	43.82	43.53	42.73	42.69	42.69	42.17	43.12	43.16	42.64	42.96	43.77	42.85	42.4	41.85	41.57	41.17	42.7	42.75	42.12
Gd	174.4	175.9	176.3	175.2	176	172.6	177.9	176.1	173.3	175.1	172.7	172.3	174.1	175.4	175.8	172.1	170.8	167.2	166.2	175.8	178	172.1
Tb	21.52	21.82	21.51	21.72	21.84	21.44	21.74	21.38	21.3	21.69	21.44	21.42	21.5	21.71	21.79	20.94	21.07	20.8	20.6	21.41	21.53	21.23
Dy	121.3	123.1	121.4	122.4	123	121.7	122.5	121.8	119.8	123.3	120.9	121.9	121.6	122.2	122.7	121.4	119.7	117.6	117.7	122.3	122.8	119.7
Ho	21.48	22.13	22	21.79	22.21	21.7	22.12	21.68	21.5	22.12	21.96	21.73	21.98	21.84	22.11	21.46	21.28	21.14	21.09	21.59	22.2	21.34
Er	54.65	55.92	55.5	54.75	55.69	55.2	55.9	55.25	54.47	55.38	54.7	54.75	54.5	55.61	55.29	54.38	53.73	53.66	53.25	54.92	55.84	53.9
Tm	6.86	6.91	6.82	6.82	6.93	6.91	6.87	6.87	6.88	6.88	6.78	6.76	6.88	6.95	6.95	6.77	6.68	6.64	6.63	6.78	6.85	6.62
Yb	39.26	40.28	40.08	38.37	39.01	38.85	39.51	40.19	39	39.59	38.98	39.16	39.28	39.46	39.19	38.79	38.36	38.14	38.32	38.97	39.85	38.4
Lu	5.181	5.28	5.207	5.29	5.32	5.23	5.296	5.337	5.25	5.35	5.29	5.332	5.33	5.202	5.17	5.098	5.15	5.066	5.02	5.296	5.268	5.127
Y	562.5	569.2	566.1	560.7	569.3	562	563.2	557.8	560.3	573.7	559.4	562.6	563.8	561.5	569.9	552.2	558.3	555.7	551.8	568.2	571.9	562.3
Sr	1553	1553	1561	1535	1550	1551	1541	1535	1552	1550	1556	1550	1559	1557	1552	1545	1529	1534	1522	1534	1540	1540
Pb	0.71	0.99	0.72	0.75	0.85	0.53	0.42	0.73	0.65	0.92	0.63	0.8	0.75	1.29	0.6	0.4	0.44	0.45	0.64	0.95	1.16	1.17
Th	23.87	24.7	23.21	24.21	24.79	23.24	24.26	23.93	22.44	25.14	23.93	24.08	23.54	24.51	24.09	23.76	23.05	23.32	22.57	24.23	25.43	22.79
U	11.65	11.96	11.18	11.61	11.83	11.23	11.72	11.69	10.97	12.09	11.58	11.53	11.47	11.62	11.55	11.44	11.23	11.32	10.92	11.48	11.79	11.06
LREE	6309.84	6389.25	6287.69	6310.12	6382.83	6261.13	6331.89	6304.59	6230.37	6384.42	6239.16	6241.34	6316.16	6319.57	6308.85	6164.70	6163.45	6181.87	6086.57	6286.70	6371.35	6215.02
HREE	270.25	275.44	272.52	271.14	274.00	271.03	273.94	272.51	268.20	274.31	270.05	271.05	271.07	272.97	273.20	268.84	265.97	263.05	262.61	271.27	274.34	266.32
LREE/ HREE	23.35	23.20	23.07	23.27	23.30	23.10	23.11	23.14	23.23	23.27	23.10	23.03	23.30	23.15	23.09	22.93	23.17	23.50	23.18	23.18	23.22	23.34
Ce/Ce*	0.96	0.96	0.96	0.97	0.97	0.98	0.96	0.97	0.97	0.98	0.94	0.97	0.96	0.96	0.97	0.96	0.97	0.97	0.96	0.96	0.98	0.98
Eu/Eu*	0.62	0.62	0.62	0.63	0.62	0.63	0.61	0.62	0.62	0.62	0.63	0.63	0.62	0.63	0.62	0.63	0.62	0.62	0.62	0.62	0.61	0.63
(La/ Yb)N	22.65	22.38	22.08	22.96	22.76	22.42	22.33	21.79	22.45	22.29	22.67	22.12	22.60	22.60	22.21	22.21	22.26	22.62	22.25	22.63	22.21	22.59
(La/ Sm)N	3.48	3.51	3.51	3.47	3.44	3.47	3.48	3.44	3.51	3.43	3.53	3.46	3.48	3.53	3.44	3.47	3.43	3.51	3.51	3.54	3.48	3.56

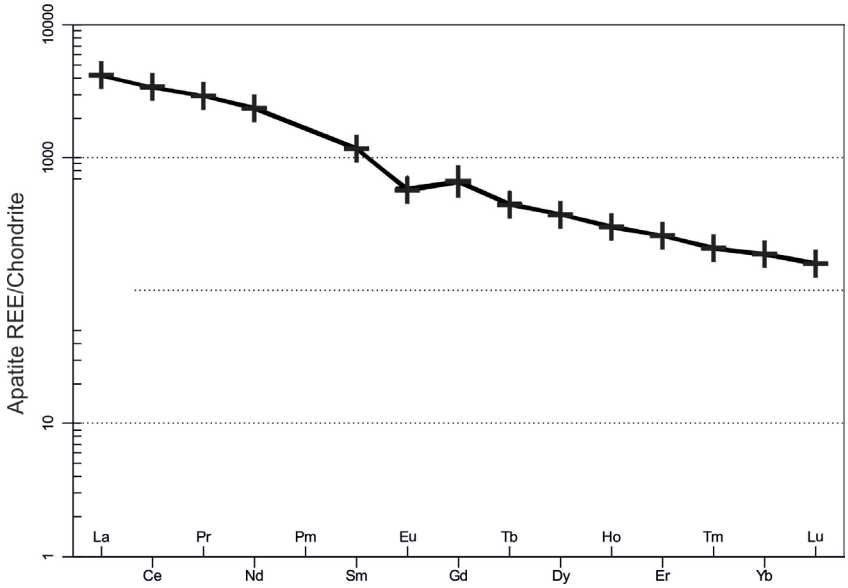

Fig. 12. Chondrite-normalized pattern for studied apatite. Chondrite values are from McDonough & Sun (1995).

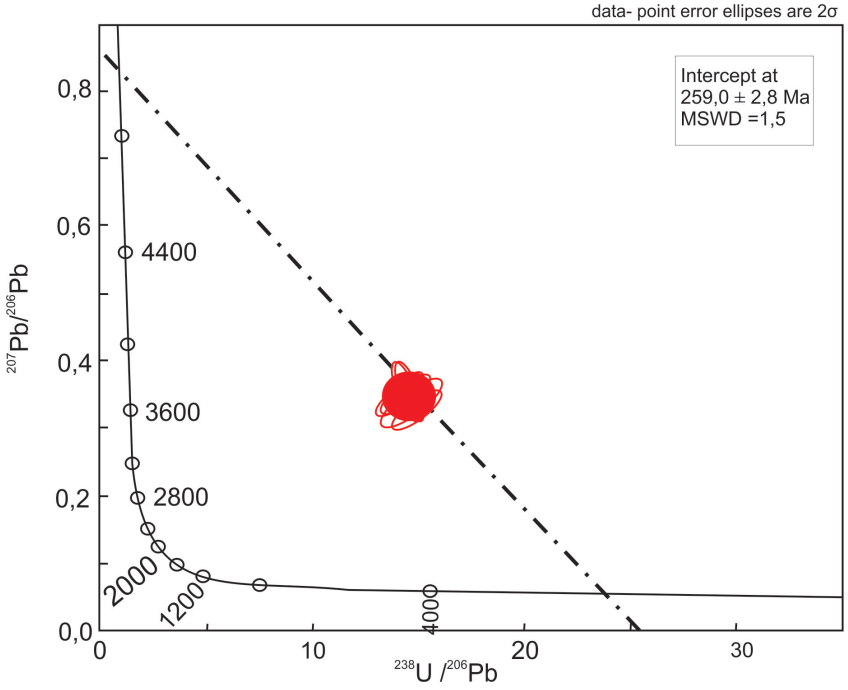

Fig. 14. The LA ICP MS analysis of apatites from the Jarabá locality.

a rather significant negative Eu anomaly can be observed. A similar course can be observed with the chondrite-normalized REE curve of bulk rocks. The contents of REE, F and Sr are similar to those found in apatites from the Frankenwald kersantites in Germany (Seifert, 2005). From secondary minerals, the chlorite, epidote and carbonates are the most common. From opaque minerals, the following association of mineral phases was found: magnetite, ilmenite (unspecified Fe-Ti oxides), rutile, hematite and pyrite. Some younger minerals (Fe-Ti oxides, hematite) supersede older mineral phases (magnetite) in the process of magmatic autohydrothermal processes (Fig. 13).

Geochronology of lamprophyres

The age of the lamprophyre rocks studied has not been precisely determined so far and their expected age classification was based on their outcropping (in crystalline rocks, they do not penetrate through the surrounding Mesozoic complexes) and the degree of alteration. In general, their age was considered as Late Paleozoic. Apatite was also used to determine the age of the rocks from Jarabá, with the aid of U/Th-Pb dating (LA ICP-MS, University of Dublin). The detected age of the rocks is 259.0 ± 2.8 Ma (Fig. 14), which stratigraphically corresponds to the

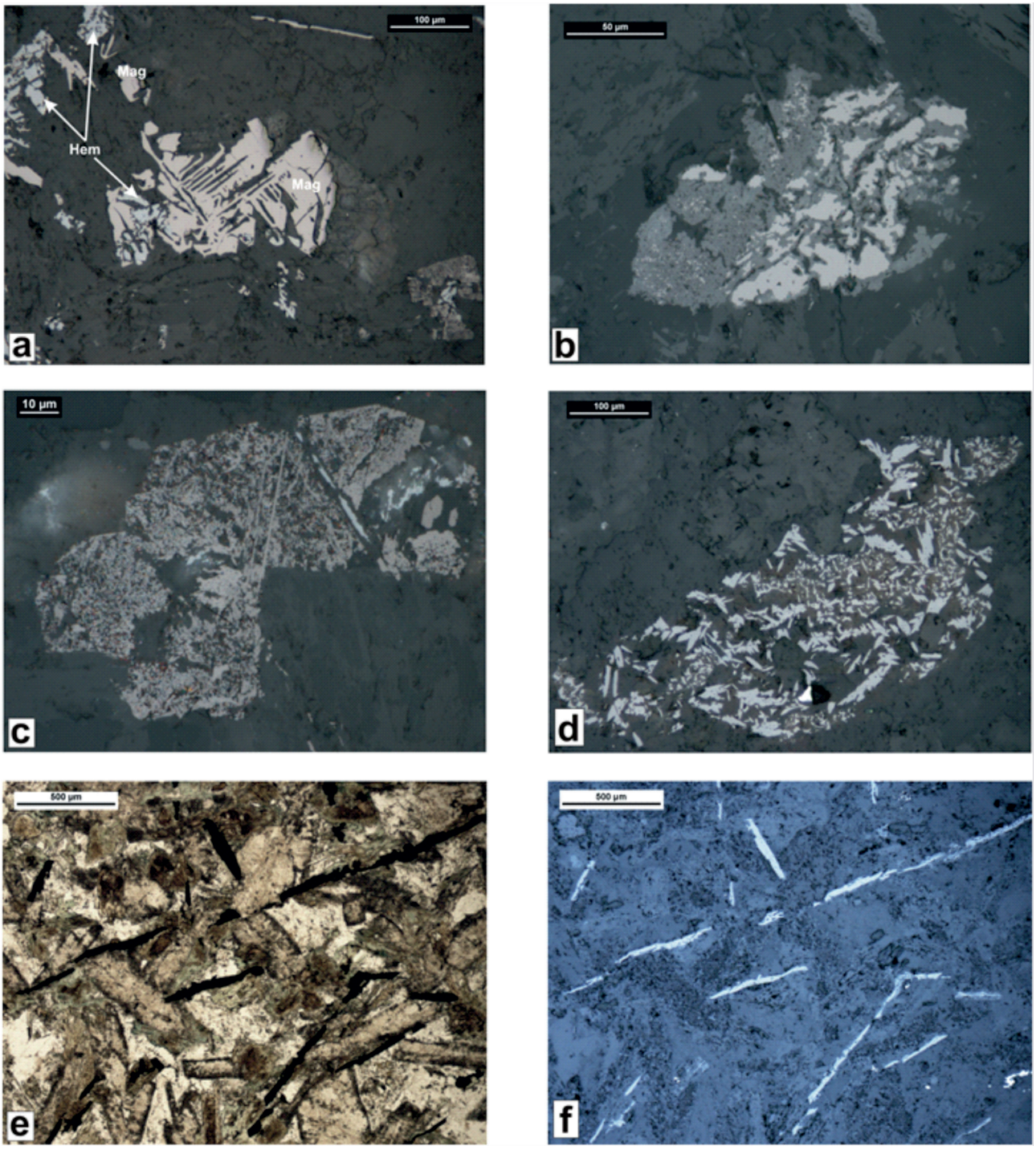

Fig. 13. The microphotography of opaque minerals: a – Disintegrated magnetite grain (Mag) pressed with hematite (Hem) and Fe-Ti oxides (dark grey) in locality of Kumštová valley, reflected light 1N. b – Relics of magnetite (Mag) form in Fe-Ti oxides (dark-grey), locality: Jarabá, reflected light, 1N. c – Leucoxenized grain of Fe-Ti oxides decomposed into mixture of rutile (Rt) and hematite (Hem) in locality Kumštová valley, reflected light, 1N. d – Phantom rutile (Rt) after the original Fe-Ti oxide grain, light grain is pyrite (Py) in locality Kumštová valley, reflected light, 1N. e – Fe-Ti oxides (black) forming strips in lamprophyre from the locality of Jarabá, transmitted light, 1N. f – Detto as in part e – Fe-Ti oxides (white) from the locality of Jarabá, reflected light, 1N.

Permian. Similar ages were also found in the lamprophyre rocks of the Považský Inovec Mts. (Pelech et al., 2017), the Malá Fatra Mts. (Spišiak et al., 2018) and the Permian volcanics of the Hronicum (Malužiná Fm.; Vozár et al., 2015).

Conclusion

Based on the mineral composition, the studied lamprophyre rocks from the southern slopes of the Nízke Tatry Mts. can be characterized as kersantites and spessartites. Lamprophyres occur within the sequence of metamorphic crystalline rocks (muscovite-biotite paragneisses) and are strongly altered. From mafic minerals, mainly clinopyroxenes, amphiboles and biotites occur in the rocks. Clinopyroxenes, by their composition, correspond to augite. Amphiboles can be classified as Ca-amphiboles – tremolites. However, their composition is strongly influenced by alteration processes. Biotites are characterized by a high content of TiO_2, indicating their magmatic origin. The felsic minerals are represented by feldspar and quartz. Among the feldspars, there are plagioclases and K-feldspars. Plagioclases have a basicity from labradorite to albite and predominate over K-feldspar. Alkaline feldspars have, in addition to various amounts of sodium (Na_2O content up to 3.72 %), often also increased contents of Ba. In some cases (BaO = 5.46 %) we can already consider the barium feldspars – hyalophane. Apatites and zircons are present in accessory amounts. Apatite corresponds to fluorine dominant type (F 4.0 wt.%), which is characteristic for orogenic calc-alkaline lamprophyre. Apatite has a high content of REE, with a significant enrichment of LREE. Secondary minerals include chlorite, epidote and carbonates. Ore minerals are represented by magnetite, ilmenite, hematite and pyrite. Based on the mineral composition of the rocks, the studied lamprophyres belong to calc-alkaline type – it well corresponds to their geochemical composition (calc-alkaline lamprophyre with affinity for orogenic – subduction related types; Spišiak et al., 2017; Vetráková & Spišiak, 2018).

The age of the studied lamprophyre rocks was determined by LA ICP-MS analysis of apatites to 259.0 ± 2.8 Ma, stratigraphically corresponding to the Permian and being in agreement with their geological position. The similarity of their mineral and chemical composition with Permian volcanics of the Hronicum and identical age point to a possible co-magmatism of these rocks.

Acknowledgements

This research was supported by grants VEGA 1/0650/15, 1/0237/18 and APVV 15-0050. We appreciate the critical reviews by Marian Putiš and anonymous reviewer who helped to improve the manuscript.

References

Abdelfadil, K. H., Romer, R. L., Seifert, T. H. & Lobst, R., 2013: Calc-alkaline lamprophyres from Lusatia (Germany) – evidence for a repeatedly enriched mantle source. *Chem. Geol., 353, 230 – 245.*

Abdel-Rahman, A. M., 1993: Nature of biotites from alkaline, calcalkaline, and peraluminous magmas. *J. Petrol., 35, 525 – 541.*

Awdankiewicz, M., 2007: Late Palaeozoic lamprophyres and associated mafic subvolcanic rocks of the Sudetes (SW Poland): petrology, geochemistry and petrogenesis. *Geol. Sudet., 39, 11 – 97.*

Belousova, E. A., Griffin, W. L., O'Reilly, S. Y. & Fisher, N. I., 2002: Apatite as an indicator mineral for mineral exploration: trace-element composition and their relationship to host rock type. *J. Geochem. Explor., 76, 45 – 69.*

Chakhmouradian, A., Reguir, E. P. & Mitchell, R. H., 2002: Strontium-apatite: New occurrences, and the extent of Sr-for-Co substitution in apatite-group minerals. *Canad. Mineralogist, 40, 121 – 136.*

Chew, D. M. & Donelick, R. A., 2012: Combined apatite fission track and U-Pb dating by LA-ICP MS and future trends in apatite provenance analysis. In: Sylvester P. (Ed.): Quantitative mineralogy and microanalysis of sediments and sedimentary rocks. *Mineral. Assoc. Canada*, 219 – 248.

Chew, D., Petrus, J. A. & Kamber, B. S., 2014: U-Pb LA-ICP MS dating using accessory mineral standards with variable common Pb. *Chem. Geol., 363, 185 – 199.*

Chu, M. F., Wang, K. L., Griffin, W. L., Chung, S. L., O'Reilly, S. Y., Pearson, N. J. & Ilzuka, Y., 2009: Apatite composition: Tracing petrogenetic processes in Transhimalayan granitoids. *J. Petrol., 50, 1 829 – 185.*

Cochrane, R., Spikings, R. A., Chew, D., Wotzlaw J. F., Chiaradia, M., Tyrrell, S., Schaltegger, U. & Van der Lelij, R., 2014: High temperature (>350 °C) thermochronology and mechanisms of Pb loss in apatite. *Geochim. cosmochim. Acta, 127, 39 – 56.*

Geologická mapa Slovenska M 1 : 50 000 [online]. Bratislava, Št. Geol. Úst. D. Štúra, 2013. Available on the internet: http://apl.geology.sk/gm50js.

Hawthorne, C. F., Oberti, R., Harlow, G. E., Maresch,V. W., Martin, F. R., Schumacher C. J. & Welch, D. M., 2012: Nomenclature of the amphibole supergroup. *Amer. Mineralogist, 97, 2 031 – 2 048.*

Hegner, E., Kölbl-Ebert, M. & Loeschke, J., 1998: Postcollisional Variscan lamprophyres (Black Forest, Germany), $^{40}Ar/^{39}Ar$ phlogopite dating, Nd, Pb, Sr isotope and trace element characteristics. *Lithos, 45, 395 – 411.*

Hovorka, D., 1967: Porphyres and lamprophyres from tatraveporide crystalline complexes. *Sbor. geol. Vied, 8, 51 – 78.*

Kamenický, J., 1962: Geological-petrographic conditions of kersantite of the Nízke Tatry Mts. *Geol. Práce, Zpr., 24.*

Krist, E., 1967: Geological-petrographic conditions of spessartite-kersantite dyke in the Nízke Tatry Mts. *Acta. geol. geogr. Univ. Comen., Geol., 12, 63 – 73.*

Krmíček, L., Cempírek, J., Havlín, A., Přichystal, A., Houzar, S., Krmíčková, M. & Gadas, P., 2011: Mineralogy and pet-

rogenesis of a Ba-Ti-Zr-rich peralkaline dyke from Šebkovice (Czech Republic): recognition of the most lamproitic Variscan intrusion. *Lithos, 121, 74 – 86.*

Ladenburger, S., Marks**, M. A. W.,** Upton, B., Hill, P., Wenzel, T. & Markl, G., 2016: Compositional variation of apatite from rift-related alkaline igneous rocks of the Gardar Province, South Greenland. *Amer. Mineralogist, 101, 612 – 626.*

Le Maitre, R. W., Streckeisen, A., Zanettin, B., Le Bas, M. J., Bonin, B., Bateman, P., Bellieni G., Dudek, A., Efremova, S., Keller, J., Lameyre, J., Sabine, P. A., Schmidt, R., Sorensen, H. & Wolley, A. R., 2002: Igneous rocks a classification and Glossary of Terms. Recommendationas of the International Union of Geological Sciences. Subcommision on the Systematics of Igneous Rocks. *Cambridge University Press, 236 pp.*

Macdonough, W. F. & Sun, S. S., 1995*:* Composition of the Earth. *Chem. Geol., 120, 228.*

McDowell, F.W., McIntosh, W. C. & Farley, K. A., 2005: A precise ^{40}Ar-^{39}Ar reference age for the Durango apatite (U-Th)/He and fission-track dating standard. *Chem. Geol., 214, 249 – 263.*

Mitchell, R. H. & Bergman, S. C., 1991: Petrology of Lamproites. *New York, Plenum. Press, 1 – 447.*

Morimoto, N., Fabries, J., Ferguson, A. K., Ginzburg, I. V., Ross, M., Seifert, F. A., Zussman, J., Aoki, K. & Gottardi, G., 1988: Nomenclature of pyroxenes. *Amer. Mineralogist, 73, 1 123 – 1 133.*

Ondrejka, M., Huraiová, M., Petrík, I., Kohút, M., Spišiak, J., Šarinová, K., Konečný, V. & Vančová, I., 2015: Klasifikácia a nomenklatúra magmatických hornín. *Miner. Slov., 47, 97 – 112.*

Pandey, R., Chalapathi Rao, N. V., Dhote, P., Pandit, D., Choudhary, A. K., Sahoo, S. & Lehmann, B., 2017: Rift-associated ultramafic lamprophyre (damtjernite) from the middle part of the Lower Cretaceous (125 Ma) succession of Kutch, northwestern India: Tectonomagmatic implications. *Geosci. Front., 1 – 20.*

Paton, C., Hellstrom, J., Paul, B., Woodhead, J. & Hergt, J., 2011: Iolite: freeware for the visualisation and processing of mass spectrometric data. *J. Anal. At. Spectrom., 26, 2 508 – 2 518.*

Pelech, O., Vozárová, A., Uher, P., Petrík, I., Plašienka, D., Šarinová, K. & Rodionov, N., 2017: Late Permian volcanic dykes in the crystalline basement of the Považský Inovec Mts. (Western Carpathians): U-Th-Pb zircon SHRIMP and monazite chemical dating. *Geol. Carpath., 68, 6, 530 – 542.*

Petrus, J. A. & Kamber, B. S., 2012: Vizual age: A novel approach to laser ablation ICP-MS U-Pb geochronology data reduction. *Geostand. Geoanalytical. Res., 36, 247 – 270.*

Plank, T. & Langmuir, C. H., 1998: The chemical composition of subducting sediment and its consequences for the crust and mantle. *Chem. Geol., 145, 325 – 394.*

Rieder, M., Cavazzini, G., D'Yakonov, Y. S., Frank-Kamenetskii V. A., Gottardi, G., Guggenheim, S., Koval, P. V., Müller, G., Neiva, A. M. R., Radoslovich, E. W., Robert, J. L., Sassi, F. P., Takeda, H., Weiss, Z. & Wones, D. R., 1998: Nomenclature of micas. *Canad. Mineralogist, 36, 905 – 912.*

Schoene, B. & Bowring, S. A., 2006: U-Pb systematics of the McClure Mountain syenite: thermochronological constraints on the age of the ^{40}Ar/^{39}Ar standard MMhb. *Contr. Mineral. Petrology, 151, 5, 615 – 630.*

Seifert, T., 2008: Metallogeny and Petrogenesis of Lamprophyres in the Mid-European Variscides. *Amsterdam, IOS Press Millpress, 1 – 303.*

Seifert, W., 2005: REE-, Zr-, and Th-rich titanite and associated accessory minerals from a kersantite. *Mineral. Petrol., 84, 129 – 146.*

Spišiak, J., Vetráková, L., Chew, D., Ferenc, Š., Šimonová, V. & Prokešová, R., 2017: Calc-alkaline laprophyres from Nízke Tatry Mts. *13th Workshop of Alpine Geological Studies. Serbia, 100 pp.*

Spišiak, J., Vetráková, L., Chew, D., Ferenc, Š., Mikuš, T., Šimonová, V. & Bačík, P., 2018: Petrology and dating of the Permian lamprophyres from the Malá Fatra Mts. (Western Carpathians, Slovakia). *Geol. Carpath., 69, 5, 453 – 466.*

Štemprok, M., Dolejš, D. & Holub, F. V., 2014: Late Variscan calc–alkaline lamprophyres in the Krupka ore district, Eastern Krušné Hory/Erzgebirge: their relationship to Sn-W mineralization. *J. Geosci., 59, 41 – 68.*

Tappe, S., Foley, S. F., Jenner, G. A., Heaman, L. M., Kjarsgaard, B. A., Romer, R. L., Stracke, A., Joyce, N. & Hoefs, J., 2006: Genesis of ultramafic lamprophyres and carbonatites at Aillik Bay, Labrador: a consequence of incipient lithospheric thinning beneath the North Atlantic Craton. *J. Petrology, 47, 1 261 – 1 315.*

Thomson, S. N., Gehrels, G. E., Ruiz, J. & Buchwaldt, R., 2012: Routine low-damage apatite U-Pb dating using laser ablation-multicollector-ICPMS. *Geochem. Geophys. Geosyst*., 13, 2, 23.

Turpin, L., Velde, D. & Pinte, G., 1988: Geochemical comparison between minettes and kersantites from the western European Hercynian orogen: trace element and Pb-Sr-Nd isotope constraints on their origin. *Earth. planet. Sci. Lett., 87, 73 – 86.*

Ulrych, J., Pivec, E., Zak, K., Bendl, J. & Bosak, P., 1993: Alkaline and ultramafic carbonate lamprophyres in central Bohemian carboniferous basins, Czech Republic. *Mineral. Petrol., 48, 65 – 81.*

Vetráková, L. & Spišiak, J., 2018: Geochemistry and geochronology of calc-alkaline lamprophyres, Central Slovakia/Western Carpathians. *Joint 5th Central-European Mineralogical Conference and 7th Mineral Sciences in the Carpathians Conference, 112 pp.*

Vozár, J., Spišiak, J., Vozárová, A., Bazarník, J. & Kráľ, J., 2015: Geochemistry and Sr, Nd isotopic composition of the Hronic Upper Paleozoic basic rocks (Western Carpathians, Slovakia). *Geol. Carpath., 66, 3 – 17.*

Mineralógia a geochronológia vápenato-alkalických lamprofýrov z Nízkych Tatier (tatrikum, Západné Karpaty)

Lamprofýry sú dajkové horniny, ktoré sú minerálnym zložením, štruktúrou a do určitej miery aj chemickým zložením odlišné od intruzívnych a efuzívnych hornín. Ide o tmavozelené porfyrické horniny s jemnozrnnou až afanitickou základnou hmotou. V kryštaliniku Nízkych Tatier bolo opísaných viacero telies týchto bázických žilných hornín (Kamenický, 1962; Hovorka, 1967; Krist, 1967). Pri štúdiu sme sa zamerali na relatívne najčerstvejšie typy hornín z dvoch lokalít: z oblasti Jarabá – Mýto pod Ďumbierom; 1 – odkryv pri ústí Kumštovej doliny nad hlavnou cestou na Čertovicu, N 48° 54′ 19″, E 19° 42′ 14″; 2 – starší opustený lom zhruba v strede dediny Jarabá na ľavej strane potoka, N 48° 53′ 25″, E 19°, 41′ 39″. Telesá žilných hornín na lokalite Jarabá a Kumštová dolina ležia v rulách (staršie paleozoikum). Študované lamprofýrové horniny z Nízkych Tatier na základe klasifikácie IUGS (Le Maitre et al., 2002; Ondrejka et al., 2015) zaraďujeme na lokalite Kumštová dolina ku kersantitom a na lokalite Jarabá k spessartitom. Minerálne zloženie tvoria primárne (mafické a felzitické), sekundárne a opakové minerály. Z mafických minerálov sa v horninách vyskytujú hlavne klinopyroxény, amfiboly a biotity. Z felzitických minerálov sú prítomné živce a kremeň. Klinopyroxény svojím zložením zodpovedajú augitom (Morimoto et al., 1988), amfiboly Ca-amfibolom, tremolitom (Hawthorne et al., 2012). Ich koexistencia s klinopyroxénmi je však nejasná a sú pravdepodobne mladšie. Pre biotity je charakteristický vysoký obsah TiO_2, čo poukazuje na ich magmatický pôvod. Zo skupiny živcov sa vyskytujú plagioklasy aj draselné živce. Plagioklasy majú bazicitu zodpovedajúcu labradoritu a po okrajoch ich zatláča mladší albit. Alkalické živce okrem rôzneho zastúpenia sodíka (obsah Na_2O do 3,72 %) majú často aj zvýšený obsah Ba. V niektorých prípadoch (BaO = 5,46 hm. %) už môžeme hovoriť o bárnatých živcoch. Zo sekundárnych minerálov sú zastúpené chlorit, epidot a karbonáty. Z rudných minerálov sa zistila nasledujúca asociácia opakových minerálnych fáz: magnetit, ilmenit (resp. nešpecifikované Fe-Ti oxidy), rutil, hematit a pyrit. Vek študovaných lamprofýrových hornín bol stanovený LA ICP-MS analýzou apatitov a je 259,0 ± 2,8 Ma.

Doručené / Received: 1. 4. 2019
Prijaté na publikovanie / Accepted: 4. 6. 2019